A pillared layer MOF with anion-tunable magnetic properties and photochemical [2 + 2] cycloaddition†

Xin-Yi Wang, Zhe-Ming Wang and Song Gao*

Received (in Cambridge, UK) 13th November 2006, Accepted 19th January 2007
First published as an Advance Article on the web 8th February 2007
DOI: 10.1039/b616516h

A magnetic MOF with two distinct functions was prepared and characterized: [2 + 2] photodimerization and antiferromagnetism with a well-pronounced anion-tunable spin–flop transition below 2.5 K were both observed.

Molecular materials with two or more properties, such as porosity, conductivity, photoactivity, and magnetism have recently attracted intense interest because these so-called multifunctional materials offer the possible synergism of different functions and thus new potential applications.[1] Hybrid *m*etal-*o*rganic *f*rameworks (MOFs), where the inorganic and organic parts can both contribute different properties, provide one good approach to these materials.[1,2] Concerning photochemical and magnetic properties, light-induced spin crossover behavior known as LIESST and photo-induced magnetism of Prussian blue analogs are the two most well known examples.[1b,3] Both of them use photons which interact primarily with the inorganic part (metal ions) to modify the magnetic properties. For porosity and photoactivity, despite the abundant investigations of homochiral catalysis and enantioselective separation in the inorganic porous materials, only a few studies have looked at reactions which occur in MOF cavities.[4] Of crystalline compounds containing two or more distinct channels[5] there are only four examples. One such compound, which was reported very recently, has interesting channel-selective and independent sorption of hydrophilic and hydrophobic molecules.[5d] In light of the aspects mentioned above, we report here a multifunctional MOF $Mn_2(HCOO)_3(4,4'\text{-bpe})_3(H_2O)_3(ClO_4)$ **1** (4,4′-bpe = 4, 4′-bipyridylethylene) with two distinct functions: magnetic properties and photoreactivity. Although it is not a real porous MOF, there exist two pseudo-cavities in the framework, one of which acts as a single-molecule container for the photodimerization of 4,4′-bpe to tpcb (tpcb = tetrakis(4-pyridyl)cyclobutane) and the other can be selectively filled by anions of variable size, which remarkably can tune its magnetic properties. Magnetic studies on an oriented single crystal of **1** reveal the antiferromagnetism with a well-pronounced spin–flop transition below T_N = 2.5 K.

Single crystals of **1** were grown by evaporation of a DMF–H_2O solution of $Mn(CHOO)_2{\cdot}2H_2O$, $NaClO_4$, and 4,4′-bpe in a 1 : 1 : 1 molar ratio.‡ The 3D framework possesses Mn–HCOO–H_2O herringbone layers along the *ab* plane pillared by 4,4′-bpe, with ClO_4^- anion and lattice 4,4′-bpe residing in between (Fig. 1). The structure contains two unique octahedral Mn^{2+} ions, Mn1 and Mn2. Both metal ions are equatorially coordinated by four O atoms from three different formates and one water, with Mn–O distances of 2.11–2.19 Å, and are axially coordinated by two N atoms from two 4,4′-bpe with slightly longer Mn–N distances of 2.25 to 2.30 Å. The formates show two different bridging modes: *syn–anti* for O1–C1–O2 and O5–C3–O6, and *anti–anti* for O3–C2–O4. In the layer each Mn1 has three Mn2 neighbors linked by formate, and *vice versa*, with the Mn–Mn distances being Mn1–Mn2 = 5.16 Å, Mn1–Mn2A = 6.19 Å, and Mn1–Mn2B = 6.37 Å. To the best of our knowledge, this is the first example of a metal-formate (6,3) layer observed. One lattice water molecule (O9) lies in the window of the 2D network, and forms H-bonds with the metal-coordinated water and O1 of the formate bridges (O9–O7C = 3.08, O9–O8 = 2.70, O9–O1A = 2.87 Å), resulting in dense layers. Along *c*, Mn^{2+} ions are linked by 4,4′-bpe to form infinite chains, which are symmetrically generated by *c* glides for Mn1 and inversion centers at the origin and (0,0,0.5) for Mn2. Furthermore, the lattice 4,4′-bpe molecules are also connected to each other in the *c* direction by O–H···N hydrogen bonds (N5–O7 = 2.84, N6–O7 = 2.80 Å). The interlayer Mn–Mn distances are quite long (*ca.* 14 Å) which results in **1** being a 2D magnetic system. The lattice water O9 and the staggering of

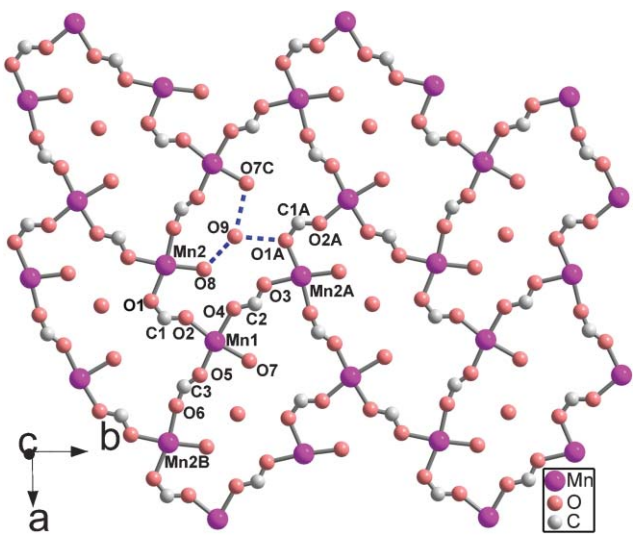

Fig. 1 The 2D herringbone layer of **1** with Mn^{2+} bridged by $HCOO^-$, hydrogen atoms are omitted for clarity. Symmetry code: A = $-x$, y + ½, $-z$ + ½; B = x + 1, y, z; C = x − 1, y, z.

Beijing National Laboratory for Molecular Sciences, State Key Laboratory of Rare Earth Materials Chemistry and Applications, College of Chemistry and Molecular Engineering, Peking University, Beijing, 100871, P. R. China. E-mail: gaosong@pku.edu.cn

† Electronic supplementary information (ESI) available: Synthetic procedure for **1** and full experimental details, solid-state photoreaction of **1**, XRD patterns of **1** before and after the photoreaction, additional structural and magnetic figures. See DOI: 10.1039/b616516h

adjacent layers blocks all possible channels of the framework and leads to the formation of two distinct pseudo-cavities in sites *A* and *B* (Fig. 2 and Fig. S1†).

Site *A*, surrounded by three 4,4′-bpe pillars, contains the ClO_4^- anion, which forms weak O···H–C bonds with its peripheral 4,4′-bpe. We have found that the anion can be replaced by NO_3^-, Br^-, I^-, and BF_4^- by choosing different starting materials in the synthesis, but is not exchangeable *in situ*. This is reasonable for the non-accessible *A* site. These anions with different sizes can subtly influence its structure, and thus its magnetic properties. Site *B*, occupied by a lattice 4,4′-bpe, is surrounded by four 4,4′-bpe pillars in a manner such that two pairs of 4,4′-bpe are nearly orthogonal to each other. The lattice 4,4′-bpe is face-to-face to one pair of the 4,4′-bpe of the box but edge-to-face to another. The former leads to parallel stacking 4,4′-bpe columns along the *b* axis (Fig. 2c). The olefins of adjacent 4,4′-bpe (C=C groups) are roughly parallel with the C–C distances being 3.883 to 4.143 Å.

This structural feature provides us a good opportunity to study the UV-induced [2 + 2] cycloaddition of 4,4′-bpe because the 4,4′-bpe columns satisfy the geometric criteria of Schmidt for [2 + 2] photodimerization, namely, parallel alignment and olefin separation of <4.2 Å.[6] UV irradiation of the crystalline sample of **1** for 2 d indicates that **1** is photoactive involving 4,4′-bpe to give 4,4′-tpcb. ^{1}H NMR shows a new set of peaks at 4.64 ppm for the CH–CH protons in 4,4′-tpcb (solvent: d_6-DMSO) which confirms the reaction.§ The yield was estimated to be less than 60% from the integral intensity of the peaks in NMR. Although this kind of reaction in the solid-state has been achieved by MacGillivray, Vittal, and others who utilized the strength and directionality of the hydrogen bonds and/or the coordination bonds to align the double bonds in appropriate positions,[7] realization of it in a magnetic MOF is quite new. Even though the XRD patterns of **1** remained almost unchanged after the irradiation (Fig. S2†), we did not accomplish the reaction from single crystal to single crystal because the reaction results in the cracking of the crystals.

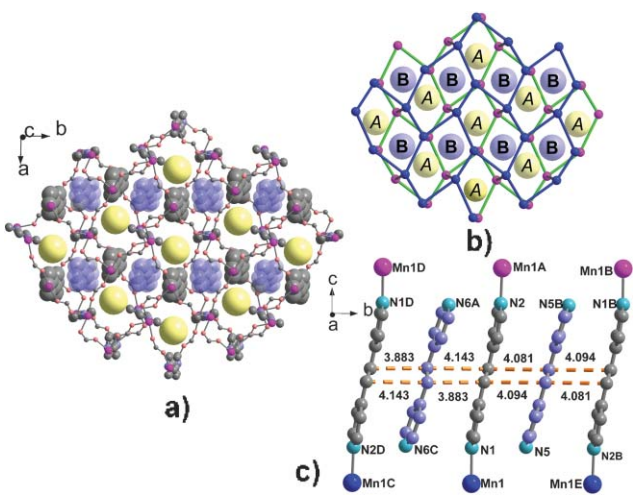

Fig. 2 (a) The pillared framework of **1**; (b) the schematic *A* and *B* sites in the framework; (c) the 4,4′-bpe column along the *b* axis. Symmetry code: A = $x, -y - ½, z - ½$; B = $-x + 1, -y + 1, -z + 1$; C = $-x + 1, y, -z + ½$; D = $1 - x, -y, 1 - z$; E = $1 - x, y + ½, -z + ½$.

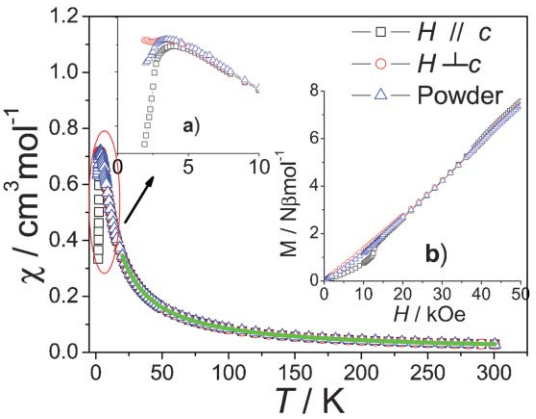

Fig. 3 Temperature dependence of χ. Inset: (a) expansion of χ below 10 K; (b) field dependent magnetization at 2 K. The data are for a single crystal ($H \parallel c$ and $H \perp c$) and a powder sample. The green line is the best-fit using HTS model (see text and ESI†).

The magnetic data per $[Mn_2]$ for an oriented single crystal with the external field $H \parallel c$ and $H \perp c$ are displayed in Fig. 3, together with that of a powder sample. Above 10 K, all $\chi(T)$ curves superpose together, reflecting the isotropic ^{6}A ground state of Mn^{2+}. Below 5 K, a significant anisotropy emerges (Fig. 3, inset a). $\chi_\parallel$ shows a pronounced peak at 3.5 K and decreases toward zero as the temperature approaches 2 K. Otherwise, $\chi_\perp$ remains almost constant after reaching the maximum at 3.5 K. Meanwhile, χ_{powder} shows a peak at 3.5 K and reaches 0.63 cm^3mol^{-1} at 2 K, close to the value 0.59 cm^3mol^{-1} of $(2\chi_\perp + \chi_\parallel)/3$. This behavior indicates that **1** is an antiferromagnet with *c* as the easy-axis.[8] The Néel temperature can be deduced from the peak position of $d\chi_\parallel T/dT$ to be T_N = 2.5 K. χT decreases monotonously from the room temperature value to a minimum at 2 K (Fig. S3). Fitting of χ^{-1} above 50 K with the Curie–Weiss law gives C = 8.65 $cm^3\ mol^{-1}$ K and a negative $\theta = -3.48$ K, indicating an intralayer AF coupling. Well documented examples show that the magnetic coupling mediated by *anti–anti* and *syn–anti* formates can be antiferromagnetic.[9] If we consider these two formates to transmit similar coupling, the susceptibility for the Heisenberg antiferromagnet (S = 5/2) of a (6,3) network (z = 3 and p_4 = 2, see ref. 10) can be fitted by Rushbrook and Wood's HTS model using the following equation with the Hamiltonian $H = -2J\sum_{\langle i,j\rangle} S_i \cdot S_j$:

$$\chi = \frac{Ng^2\beta^2 S(S+1)}{3k_B T}\left(1 + \sum_{n=1}^{6} C_n x^n\right)^{-1} \quad (1)$$

Where $x = J/kT_B$, and $C_1 = -17.5$, $C_2 = 110.8333$, $C_3 = -304.1111$, $C_4 = -991.8287$, $C_5 = 9346.140$, and $C_6 = 364381.4$. N, J, g, β, S, k_B and T have their usual meanings. The best fit of χ_{powder} above 20 K gives the intralayer coupling $J = -0.207$ cm^{-1} and g = 2.02 with $R = 3.1 \times 10^{-5}$ [$R = [\sum(\chi_{obs} - \chi_{calc})^2/\sum(\chi_{obs})^2]$], consistent with the results reported for Mn–O–C(R)–O–Mn interactions (−0.2 to −0.3 cm^{-1}).[9,11]

Furthermore, we measured the isothermal magnetization $M(H)$ of **1** at 2 K up to 50 kOe (Fig. 3, inset b). With $H \perp c$, the $M_\perp$ curve was almost a straight line reaching 7.55 μ_B at 50 kOe, lower than the M_s = 10 μ_B for $[Mn_2]$. In the low field region ($H <$ 10 kOe), $M_\parallel$ increases more slowly than $M_\perp$ does, and after an

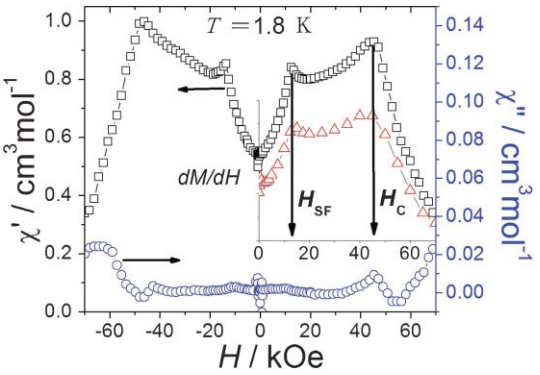

Fig. 4 The field dependence of ac susceptibility at 1.8 K of a powder sample of **1** up to 70 kOe. Inset: the derivative dM/dH of the dc magnetization.

abrupt increase, it becomes coincident with $M_{\perp}$ until the field reaches about 40 kOe, where a second change, though less pronounced, happens. These two transitions can be confirmed by the two sharp peaks in the in-phase signal of the field dependence of the ac susceptibility up to 70 kOe on a powder, which are consistent with the peaks of dM/dH (Fig. 4). This behavior is typical for a spin–flop transition, which often occurs in antiferromagnets with small anisotropy when the external field is parallel to the easy-axis. From Fig. 4, the critical fields for the transition at 1.8 K are determined to be H_{SF} = 12.8 kOe and H_c = 45.8 kOe.

Careful measurements, including the angular dependence of the magnetization and detailed $M(H)$ and $M(T)$ curves, will build the phase diagram in the H^c–T plane and give more intrinsic magnetic parameters of **1**. Meanwhile, we found that the magnetic properties, especially the critical fields of the spin–flop transition, are clearly dependent on the size of the anions in site A. The bigger the anion is, the smaller the H_c will be. For example at 1.8 K, H_c is 45.8 and 56.8 kOe when the anion is ClO_4^- and I^- respectively (Fig. S4†). Details of these will be reported later. Although we have investigated the magnetic properties on the irradiated sample (Fig. S5–6), the results are far from understandable: no spin–flop transition was found; the Curie constant C and magnetization M at 50 kOe both exceeded the calculated value for the [Mn_2] unit using the same molecular weight before irradiation. This might result from the unknown small byproducts besides the photochemical cycloaddition product due to the incompleteness of the photoreaction and some changes in the Mn^{2+} centers since the sample turns dark yellow in the process of irradiation.

In summary, we present here a good example of a multifunctional MOF involving two distinct properties: magnetism and photoreactivity. Solid-state [2 + 2] photodimerization and antiferromagnetism with well-defined spin–flop transition were both observed. Furthermore, there are two distinct functional sites where efforts can be made to adjust its properties. Anions of different size in site A can finely adjust the magnetic properties, especially the spin–flop critical fields. The possibility of the dynamic anion exchange and the influences of the photoreaction on the magnetism are main challenges in the future.

We acknowledge the support of the National Natural Science Foundation of China (Numbers 20221101, 20490210, and 20571005), the National Basic Research Program of China (2006CB601102), and the Research Fund for the Doctoral Program of Higher Education (20050001002).

Notes and references

‡ Anal: calcd for **1** $C_{39}H_{39}N_6ClO_{13}Mn_2$ (945.09): C, 49.56; N, 8.89; H, 4.16. Found: C, 49.17; N, 9.02; H, 4.26%. IR (single crystal, cm^{-1}): 3061 w, 1069 s, 1505 w, 1425 w, 1360 w, 1253 w, 1223 w, 1103 m, 1090 m, 1013 m, 972 w, 840 m, 828 m. Crystal data for **1**: monoclinic, $P2_1/c$, a = 10.1273(1), b = 15.3853(2), c = 27.6549(3) Å, β = 92.722(8)°, V = 4304.09(8) Å^3, Z = 4, GoF = 0.904. Data collection 3.43 ⩽ θ ⩽ 27.48 for **1** was performed at 293 K on a Nonius Kappa CCD with Mo-Kα radiation (λ = 0.71073 Å). The structure was solved by the direct method and refined by a full matrix least squares technique based on F^2 using the SHELXL 97 program, leading to a final $R1$ = 0.0470 for 569 parameters and 4561 unique reflections with ($I > 2\sigma(I)$) and w$R2$ = 0.1117 for all 9821 reflections. CCDC number 626790. For crystallographic data in CIF or other electronic format see DOI: 10.1039/b616516h

§ ^{1}H NMR peaks for the irradiated sample: δ = 8.58 (d, Py–H of 4,4′-bpe), 8.33 (d, Py–H of 4,4′-tpcb); 7.60 (d, Py–H of 4,4′-bpe), 7.55 (d, CH=CH of 4,4′-bpe), 7.20 (d, Py–H of 4,4′-tpcb), 4,64 (s, CH–CH of 4,4′-tpcb); see ESI for details.

1 For example: (*a*) M. E. Itkis, X. Chi, A. W. Cordes and R. C. Haddon, *Science*, 2002, **296**, 1443; (*b*) O. Sato, *Acc. Chem. Res.*, 2003, **36**, 692; (*c*) E. Coronado and P. Day, *Chem. Rev.*, 2004, **104**, 5419; (*d*) J. L. C. Rowsell and O. M. Yaghi, *Angew. Chem., Int. Ed.*, 2005, **44**, 4670; (*e*) S. S. Kaye and J. R. Long, *J. Am. Chem. Soc.*, 2005, **127**, 6506; (*f*) J. S. Miller and M. Drillon, *Magnetism: Molecules to Materials*, vol. I–V, Wiley-VCH, Weinheim, 2002–2005 and references therein.
2 (*a*) N. L. Rosi, J. Kim, M. Eddaoudi, B. L. Chen, M. O'Keeffe and O. M. Yaghi, *J. Am. Chem. Soc.*, 2005, **127**, 1504; (*b*) J. L. C. Rowsell and O. M. Yaghi, *Microporous Mesoporous Mater.*, 2004, **73**, 3; (*c*) S. Kitagawa, R. Kitaura and S. Noro, *Angew. Chem., Int. Ed.*, 2004, **43**, 2334 and references therein.
3 S. Decurtins, R. Pellaux, G. Antorrena and F. Palacio, *Coord. Chem. Rev.*, 1999, **190–192**, 841.
4 (*a*) J. S. Seo, D. Whang, H. Lee, S. I. Jun, J. Oh, Y. J. Jeon and K. Kim, *Nature*, 2000, **404**, 982; (*b*) A. Hu, H. L. Neo and W. Lin, *J. Am. Chem. Soc.*, 2003, **125**, 11490; (*c*) T. Uemura, K. Kitagawa, S. Horike, T. Kawamura, S. Kitagawa, M. Mizuno and K. Endo, *Chem. Commun.*, 2005, 5968; (*d*) J. T. Hupp and K. R. Poeppelmeier, *Science*, 2005, **309**, 2008.
5 (*a*) A. Monge, N. Snejko, E. Gutiérrez-Puebla, M. Medina, C. Cascales, C. Ruiz-Valero, M. Iglesias and B. Gómez-Lor, *Chem. Commun.*, 2005, 1291; (*b*) B. F. Abrahams, M. Moylan, S. D. Orchard and R. Robson, *Angew. Chem., Int. Ed.*, 2003, **42**, 1848; (*c*) O. Ohmori, M. Kawano and M. Fujita, *Angew. Chem., Int. Ed.*, 2005, **44**, 1962; (*d*) C. J. Jiang, A. Lesbani, R. Kawamoto, S. Uchida and N. Mizuno, *J. Am. Chem. Soc.*, 2006, **128**, 14240.
6 G. M. J. Schmidt, *Pure Appl. Chem.*, 1971, **27**, 647.
7 (*a*) L. R. MacGillivray, *CrystEngComm*, 2002, **4**(7), 37; (*b*) T. Friščić, D. M. Drab and L. R. MacGillivray, *Org. Lett.*, 2004, **6**, 4647; (*c*) N. L. Toh, M. Nagarathinam and J. J. Vittal, *Angew. Chem., Int. Ed.*, 2005, **44**, 2237; (*d*) Q. L. Chu, D. C. Swenson and L. R. MacGillivray, *Angew. Chem., Int. Ed.*, 2005, **44**, 3569; (*e*) D. B. Varshney, X. C. Gao, T. Friščić and L. R. MacGillivray, *Angew. Chem., Int. Ed.*, 2006, **45**, 646 And references there in.
8 R. L. Carlin, *Magnetochemistry*, Springer-Verlag, Berlin Heidelberg, 1986.
9 (*a*) Z. M. Wang, B. Zhang, T. Otsuka, K. Inoue, H. Kobayashi and M. Kurmoo, *Dalton Trans.*, 2004, **15**, 2209; (*b*) X. Y. Wang, H. Y. Wei, Z. M. Wang, Z. D. Chen and S. Gao, *Inorg. Chem.*, 2005, **44**, 572–583.
10 G. S. Rushbrook and P. J. Wood, *Mol. Phys.*, 1958, **1**, 257–283.
11 M. Viertelhaus, H. Henke, C. E. Anson and A. K. Powell, *Eur. J. Inorg. Chem.*, 2003, 2283–2289.